Scientific Research Publishing

Journal of Quantum Information Science, 2023, 13, 138-155
https://www.scirp.org/journal/jqis
ISSN Online: 2162-576X
ISSN Print: 2162-5751

Leveraging Quantum Computing for the Ising Model to Simulate Two Real Systems: Magnetic Materials and Biological Neural Networks (BNNs)

David L. Cao, Khoi Dinh

Thomas Jefferson High School for Science and Technology, Alexandria, VA, USA
Email: davidcao1440@gmail.com, khoiddinh@gmail.com

How to cite this paper: Cao, D.L. and Dinh, K. (2023) Leveraging Quantum Computing for the Ising Model to Simulate Two Real Systems: Magnetic Materials and Biological Neural Networks (BNNs). *Journal of Quantum Information Science*, **13**, 138-155.
https://doi.org/10.4236/jqis.2023.133008

Received: July 18, 2023
Accepted: September 9, 2023
Published: September 12, 2023

Abstract

Quantum computing is a field with increasing relevance as quantum hardware improves and more applications of quantum computing are discovered. In this paper, we demonstrate the feasibility of modeling Ising Model Hamiltonians on the IBM quantum computer. We developed quantum circuits to simulate these systems more efficiently for both closed and open boundary Ising models, with and without perturbations. We tested these various geometries of systems in both 1-D and 2-D space to mimic two real systems: magnetic materials and biological neural networks (BNNs). Our quantum model is more efficient than classical computers, which can struggle to simulate large, complex systems of particles.

Keywords

Ising Model, Magnetic Material, Biological Neural Network, Quantum Computting, International Business Machines (IBM)

1. Introduction

Over the last decade, the field of quantum computing has seen exponential growth. In 2022 alone, 2.35 billion dollars of public and private investment has been specifically dedicated to quantum technology [1]. Quantum computing has gained traction due to its unique ability to evaluate certain computations exponentially faster than the most advanced classical supercomputers [2].

Many benefits of quantum computing derive from its ability to "brute force" problems efficiently. Classical computers store information by stringing together

bits of zero or one to represent data. In contrast, quantum bits, or qubits, store a multitude of possible states as a single unit.

In essence, a qubit stores the probability of outputting 0 or 1 when measured. This probabilistic state, or superposition, allows quantum computing to store more data, and therefore, calculations with quantum computing are orders of magnitude faster compared to classical computing [3].

Quantum computing has been theoretically applied to several fields, such as cryptography. For instance, Shor's algorithm has the potential to break existing encryption algorithms like the Rivest-Shamir-Adleman (RSA) [4]. However, traditional classical computing struggles to decrypt the algorithm because doing so requires factoring large integers, a task exponential with time. On the other hand, a quantum approach known as Shor's algorithm factors integers with time complexity of $O\left(\left(\log N\right)^3 * \log\left(\log\left(N\right)\right) * \log\left(\log\left(\log\left(N\right)\right)\right)\right)$, one that is exponentially faster than the classical counterpart of $O\left(N\right)$ [5]. As quantum computers mature and become more reliable, quantum algorithms will in turn become more applicable and significantly change the way information is processed [3].

In this paper, we paired quantum computing with the Ising Model. The Ising Model, developed by Ernest Ising, was originally theorized to study phase transitions of different ferromagnetic materials [6]. Over time, the influence of the Ising Model grew. Currently, there exist applications of the Ising Model in tandem with quantum computing. One particular application incorporates the adiabatic theorm, which uses a specific Ising Model with the Variational Quantum Eigensolver (VQE) to solve combinatorial problems such as the social worker's problem [7]. Another uses the Ising Model with spin $S = 1$, the equilibrium model, to simulate tax evasion [8]. These models show the great potential for the intersection of quantum computing and the Ising Model. Our research in this paper emphasizes this idea.

The building blocks of the Ising Model are two-level binary quantum particles, such as electrons with spin 1/2. Groups of these electrons in a particular configuration forms what is known as the Ising Model where the spins of neighboring (adjacent) electrons affect each other's spins in a certain manner [9]. The general structure of an Ising Model can be defined in different dimensions. In this paper, we analyze applications of both the 1-D and 2-D Ising Model. The 1-D Ising Model simply represents chains of electrons in a linear space. Indeed, the 1-D Ising Model may differ depending on the specific application. The primary distinction between subsets of the 1-D Ising Model is whether or not the first and last electrons interact. If they do interact, the particular Ising Model is closed, and if they do not interact, the particular Ising Model is open. The 1-D Ising Model is assumed in the magnetic materials application to emphasize the idea that even a less complex model can accurately simulate real systems. On the other hand, the 2-D Ising Model represents electrons in a plane-like configuration [10]. In this paper, we applied a 2-D tree-like Ising Model to simulate a bio-

logical neural network.

Upon reading the abstract and this far in the introduction, a question that may naturally occur is *how the Ising Model relates to magnetic materials or BNNs, the two applications of the Ising Model explored in this paper.*

The answer to this question boils down to what an electron and its respective spin represent in the realm of quantum computing. The Ising Model can be mathematically represented by the Hamiltonian, which quantifies the total energy of a given system [11]. In quantum computing, the Hamiltonian can be represented by a quantum circuit composed of a series of qubits acted on by operators. Every electron in the Ising Model can be seen as a qubit in a quantum circuit because qubits and electrons are both inherently binary constructs [12]. In quantum circuits, interactions between adjacent electrons are therefore represented by quantum gates that alters a qubit's direction of spin. Running a correctly constructed quantum circuit produces data revealing the probabilities of each qubit or electron having an upward or downward spin [13]. This paper illustrates that this probabilistic data alone is enough to analyze an Ising Model that maps to a real life system.

In this paper the idea is straightforward. We demonstrate the applicability of the Ising Model when paired with quantum computing. We do this by simulating both magnetic materials and biological neural networks, two important real-world systems. We demonstrate that the Ising Model is capable of classifying magnetic materials as ferromagnetic or paramagnetic based on the probabilistic qubit spin distributions from the corresponding quantum circuit. Results from the magnetic material quantum circuit ultimately show all possible electron spin configurations, including when all electrons are spin-up or spin-down. If the probability of all electrons being aligned is highest, the material is ferromagnetic, and if the probability of all electrons being misaligned is highest, then the material is paramagnetic. Ferromagnetic materials exhibit the strongest attraction towards magnets (or external magnetic fields), whereas paramagnetic materials exhibit the weakest attraction towards magnets [14]. We also show that the Ising Model, when applied to quantum computing, is able to model biological neural networks (BNNs) because neurons are either active or inactive, a binary state shared with qubits. Our model can potentially reduce neurosurgery risk because we can mathematically calculate the relative importance of each neuron. From this information, experts will be able to weigh options and therefore make better judgments prior to neurosurgery.

Overall, the motivation for the research presented in this paper was to take existing mathematical frameworks and combine them with the advantages of quantum computing to solve real-world problems. We hope that by doing so, we can advance the practicality of quantum computing and provide a solid foundation for future research.

In the next section, we delve deeper into the Ising Model and, congenially, the methodology behind simulating magnetic materials and neural networks. Fol-

lowing the methodology, we will analyze the results produced by the quantum circuits in both applications. Finally, we will conclude with a discussion of our results and their significance.

2. Methodology

Simulating any particular real system using a unique Ising Model requires following a series of steps shown below.

1) Alter the "base" Ising Model as needed to match the properties of the chosen physical system. This so-called "base" Ising Model will be defined thoroughly in Section 2.1.

2) Mathematically describe the chosen system's Ising Model with a Hamiltonian *H*.

3) Represent the Ising Model on a quantum circuit (we used IBM) [13].

4) Run the quantum circuit and use the probabilistic results to analyze the chosen physical system.

2.1. Base Ising Model

The aforementioned "base" Ising Model is a 1-D open model and is its energy, *H*, is commonly denoted by the following mathematical expression

$$H = \frac{-J}{2}\sum_{i=1}^{N-1}\sigma_i\sigma_{i+1} + h\sum_{j=1}^{N}\sigma_j \tag{1}$$

where N is the number of particles, σ_i is the spin (between −1 and 1) of the particle with positional index i, and J and h are the interaction coefficient of the particle and the magnitude of any existing perturbations, respectively [15]. The left summation describes the interactions between electrons, and the right summation factors in any perturbations or external magnetic fields acting on the system.

Since quantum systems are time-dependent, we must time-evolve *H*. Instead of a scalar value σ representing a particle's spin, we now use the Z basis, where $Z = \begin{bmatrix} 1 & 0 \\ 0 & -1 \end{bmatrix}$ since spin can have any value between −1 and 1 [16]. Additionally, we represent perturbations as the X basis, where $X = \begin{bmatrix} 0 & 1 \\ 1 & 0 \end{bmatrix}$ [16]. We could choose a different matrix to represent perturbations so long as it differs from the Z basis. After making these changes, our mathematical model is now equivalent to Equation (2):

$$\hat{H} = \frac{-J}{2}\sum_{i=1}^{N-1}Z_iZ_{i+1} + h\sum_{j=1}^{N}X_j \tag{2}$$

However, in order to adequately implement an Ising Model on a quantum circuit, we must break down the Hamiltonian $\hat{H}$ to predefined rotation operators on a quantum circuit. Let the following be true:

$$\hat{H} = \frac{-J}{2}\sum_{i=1}^{N-1}Z_iZ_{i+1} + h\sum_{j=1}^{N}X_j = \hat{A} + \hat{B}. \tag{3}$$

The terms $\hat{A}$ and $\hat{B}$ are intelligible by a quantum circuit because the expressions can be simplified to $R_{ZZ}(\theta)$ gates (composed of *CNOT*, $R_Z(\theta)$, and *CNOT* logical operators) for interactions between neighboring particles and $R_X(\theta)$ gates for perturbations [13] [17]. For clarification, an $R_{ZZ}(\theta)$ gate performs a rotation about the z-axis across 2 qubits whereas an $R_X(\theta)$ gate performs a rotation about the x-axis across 1 qubit.

We then time-evolve the Hamiltonian by implementing the following expression: $\psi(t) = \mathrm{e}^{-i\hat{H}t/h}\psi(0)$.

Recall that $\hat{H} = \frac{-J}{2}\sum_{i=1}^{N-1} Z_i Z_{i+1} + h\sum_{j=1}^{N} X_j = \hat{A} + \hat{B}$. Since $Z_i Z_{i+1}$ does not commute with X_j, in other words, $\left[Z_i Z_{i+1}, X_j\right] \neq 0$:

$$\mathrm{e}^{-i\hat{H}t} \neq \mathrm{e}^{-i\hat{A}t}\mathrm{e}^{-i\hat{B}t} \tag{4}$$

Therefore, we cannot directly represent $\hat{H}$ on a quantum circuit, so we must apply Trotter Decomposition [17] [18]. We decompose $\mathrm{e}^{-i\hat{H}t}$ to a particular combination of $\mathrm{e}^{-i\hat{A}t}$ and $\mathrm{e}^{-i\hat{B}t}$ with minimal error [17] [18]. This particular version of Trotter Decomposition is known as the Suzuki-Trotter approximation, a direct improvement from the traditional Lie-Trotter approximation. The Suzuki-Trotter decomposition is a corollary from the Baker-Campbell-Hausdorff Zassenhaus formula, which states the following [19]:

$$\mathrm{e}^{t(X+Y)} = \mathrm{e}^{tX}\mathrm{e}^{tY}\mathrm{e}^{-\frac{t^2}{2}[X,Y]}\mathrm{e}^{\frac{t^3}{6}\left(2[Y,[X,Y]]+[X,[X,Y]]\right)\cdots} \tag{5}$$

Hence, for $\hat{H} = \hat{A} + \hat{B}$, Suzuki-Trotter decomposition states the following:

$$\mathrm{e}^{-i\hat{H}t} = \mathrm{e}^{-i\hat{A}/2t}\mathrm{e}^{-i\hat{B}t}\mathrm{e}^{-i\hat{A}/2t} + O\left(t^3\right) \tag{6}$$

The error $O\left(t^3\right)$ is negligible for our purposes. Shown below is the final mathematical expression for the open 1-D Ising Model Hamiltonian

$$\hat{H} = \hat{A}/2 + \hat{B} + \hat{A}/2 \tag{7}$$

in that specific order. We used this expression as the base model for our quantum circuits in both the magnetic material and neural network applications.

2.2. Magnetic Material Model

For the magnetic materials application, we simulate the effect of perturbations on a chain of electrons. Recall Equation (2). To do this, we alter the values of *J*, the interaction coefficient between electrons, and *h*, the perturbations coefficient. We want to determine if the values of *J* and *h* have implications on the alignment probabilities of electrons in a given system, which influences whether the system is ferromagnetic or paramagnetic. We also model a chain of electrons that wraps around in a circle, known as a closed model. The closed model is more realistic because it closely represents a real system, but its glaring drawback is the increased complexity compared to the open model. Overall, in this paper, we show the feasibility of accurately modeling ferromagnetic and paramagnetic systems using the open 1-D Ising Model. See **Figure 1** for an image showing the differences between an open and closed Ising Model.

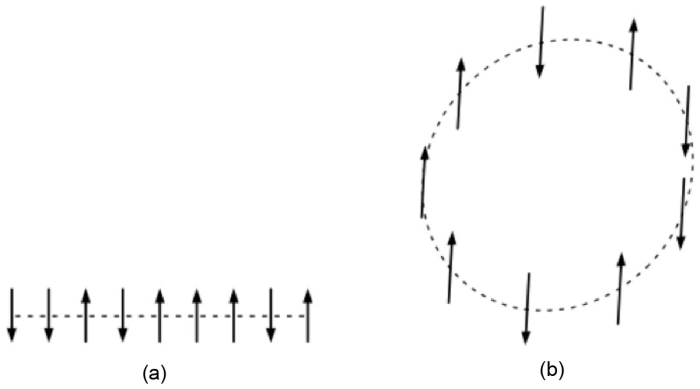

Figure 1. Open (a) and closed (b) 1-D Ising Model. The open model is merely a linear chain as the first and last electron do not interact, while the closed model is a loop where the first and last electron do interact [20].

Mathematically, for a linear chain of electrons, the Hamiltonian remains the same as that of the base Ising Model (refer to **Figure 1(a)**).

$$\hat{H} = \frac{-J}{2}\sum_{i=1}^{N-1} Z_i Z_{i+1} + h\sum_{j=1}^{N} X_j \tag{8}$$

For the closed model, since the first and last electrons interact (refer to **Figure 1(b)**)

$$\hat{H} = \frac{-J}{2}\sum_{i=1}^{N-1} Z_i Z_{i+1} + Z_N Z_1 + h\sum_{j=1}^{N} X_j \tag{9}$$

The additional term, $Z_N Z_1$, quantifies the spin interaction between the Nth electron, the last in the chain, and the 1st electron at the beginning of the chain.

2.3. Biological Neural Network Model

In addition to magnetic materials, we applied the Ising Model to more complex geometries such as biological neural networks. We modified the coefficient of interaction J and coefficient of perturbation h to develop a high-level simulation of a human BNN. In this geometry, we included a main branch and 4 different auxiliary branches which stems from the main branch.

In order to differentiate the main branch from the auxiliary branches, we increased J on the main branch. In this paper, we evaluate how changing the ratio of J_{main} and J_{aux} impacted the information retention of the system, which is quantified by entropy. We also showed how removing or damaging certain neurons affect the overall entropy of the neural network, which provides useful information regarding the relative importance of each neuron and therefore which to avoid during neurosurgery. See **Figure 2** for an image showing a particular neural network with four neurons per branch. Note the Main Branch, Central Qubit of Contact, Central Nervous System, Peripheral Nervous System, and Auxiliary Branches.

Since the BNN is a 2-D tree-like structure, the Hamiltonian of the entire system is the summation of the Hamiltonian for each branch.

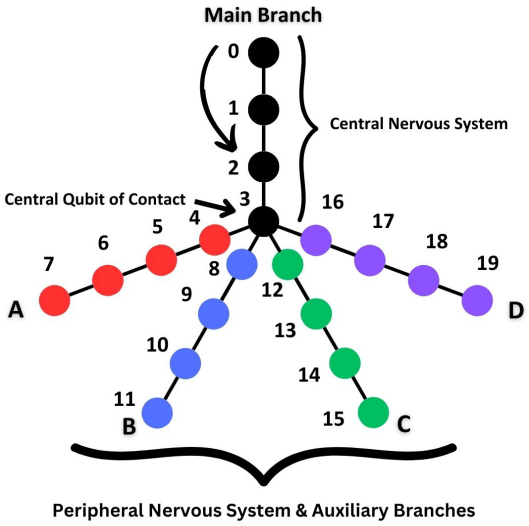

Figure 2. Biological neural network model showing the Main Branch, Central Qubit of Contact (Neuron 3), Central Nervous System, the Peripheral Nervous System, and the Auxiliary Branches (A, B, C, D). Each colored node represents a qubit that maps to a neuron in the biological neural network (BNN). Each neuron is also numbered, with indices increasing from top to bottom, left to right.

$$\hat{H} = \hat{H}_{main} + Z_n Z_1^A + Z_n Z_1^B + Z_n Z_1^C + Z_n Z_1^D + \hat{H}_A + \hat{H}_B + \hat{H}_C + \hat{H}_D \tag{10}$$

where n is the last neuron in the Main Branch. The Hamiltonian for each branch, denoted by $\hat{H}_{main}$, $\hat{H}_A$, $\hat{H}_B$, $\hat{H}_C$, and $\hat{H}_D$, are evaluated using the base Ising Model discussed in Section 2.1. Note that because we do not consider perturbations for the biological neural network model, the X basis summation in the base Ising Model equates to 0. The Suzuki-Trotter decomposition is therefore not necessary for our purposes. Hence, $\hat{H}_{main}$, $\hat{H}_A$, $\hat{H}_B$, $\hat{H}_C$, and $\hat{H}_D$ simply represent series of the following:

$$\hat{H} = \frac{-J}{2} \sum_{i=1}^{N-1} Z_i Z_{i+1} \tag{11}$$

where N is the length of said branch.

3. Main Results

3.1. Quantum Circuit Generation

In order to create a quantum circuit that maps to an Ising Model, we develop an algorithm so that variations e.g. the number of neurons in the biological neural network application are automatically or can be easily accounted for with minimal changes.

Recall that the number of qubits in the quantum circuit is equivalent to the number of particles in the system. After each qubit is initialized and prepared for rotation, we begin processing the algorithm.

The algorithm depends on the specific application. Since the Ising Model is 1-D for the magnetic materials application, we use a basic for-loop to generate

the quantum circuit. However, the BNN application is far more complex due to its 2-D tree-like structure. The algorithm for biological neural network involves first generating the branches for the tree, which is easily done with for-loops with boundaries based on the length of each branch (or the number of neurons or particles on that branch). If the length of the main branch differs, we simply modify the algorithm to append the main branch separately. While generating the tree, each neuron is simultaneously numbered as $R_{ZZ}(\theta)$ gates are inputted in their respective locations to the quantum circuit. See the pattern for the enumerated neurons in **Figure 2**. To join each branch of the tree, we use the Breadth First Search (BFS) algorithm that connects the child of the main branch to the parent of each auxiliary branch [21]. At the same time, $R_{ZZ}(\theta)$ gates are inputted into the quantum circuit.

See **Figure 3** for a visual diagram describing the quantum circuit generation process as a whole.

3.2. Quantum Circuits

Figure 4 shows a diagram of a typical magnetic material system with 2 electrons. Each purple circle represents an electron, and the blue arrow represents internal interactions between those electrons that affects their spins. **Figure 5** shows the system's corresponding quantum circuit.

In **Figure 5**, the light red squares with "H" represent the Hamiltonian operators that initialize each qubit, the red vertical lines represent the $R_{ZZ}(\theta)$ operators, the dark red squares with "RX" represents the $R_X(\theta)$ operators, and the two gray squares measures the spin probabilistic results. Recall that $R_{ZZ}(\theta)$ operators quantify interactions between electrons and $R_X(\theta)$ operators quantify

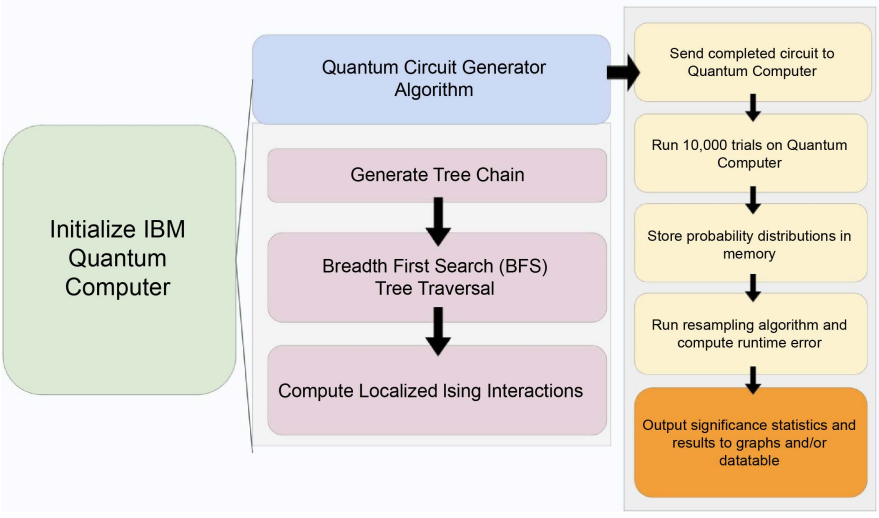

Figure 3. Quantum circuit generation algorithm using IBM Quamtum. The International Business Machines (IBM) Quantum Computer is first initialized, then the Breadth First Search (BFS) tree algorithm is used to insert the circuit operators. Finally, after running the circuit, the quantum circuit outputs probabilistic results describing all possible qubit states.

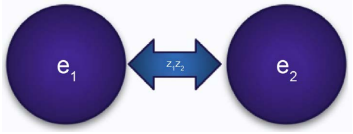

Figure 4. Hypothetical magnetic material model with 2 electrons. The blue arrow demonstrates the spin interaction between these two adjacent electrons, and each electron is indexed from 1 to N, where N is the total number of electrons in the magnetic material model.

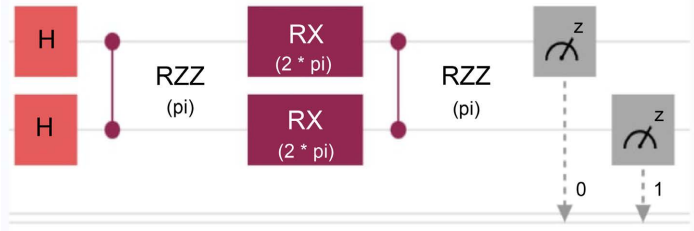

Figure 5. Hypothetical quantum circuit for a magnetic material model with 2 electrons. Note the Hamiltonian, the $R_{ZZ}(\theta)$ operators, the $R_X(\theta)$ operators, and the final measurements.

any perturbations or external magnetic field acting on the system. Also recall that in Section 2.1 Equation (5), after applying Trotter Decomposition, $\hat{H} = \hat{A}/2 + \hat{B} + \hat{A}/2$. That is why there are two $R_{ZZ}(\theta)$ operators with phase angles half of that of the $R_X(\theta)$ gates.

In this application, the results of the quantum circuit are the probabilities of measuring each electron spin configuration and therefore the probability of each electron being spin up or down. An example of an electron configuration is 01, where 0 means the left electron was measured spin-up and 1 means the right electron was measured spin-down.

The expression under the $R_{ZZ}(\theta)$ operator is its phase angle θ_{RZZ} where $\theta_{RZZ} = \frac{2\pi}{J}$. The value of J in this particular circuit is 2. Similarly, the expression under the $R_X(\theta)$ operator is also its phase angle, where $\theta_{RX} = \frac{2\pi}{h}$. The value of h in this particular configuration is 1.

Figure 6 shows a diagram of a biological neural network with 2 neurons per branch. The Main Branch is black and the two Auxiliary Branches are red and blue. Each neuron is indexed from 0 to N where N is the number of neurons in the neural network. Figure 7 shows the system's corresponding quantum circuit.

In Figure 7, the light blue squares represent the initialized Hamiltonian operators, the purple vertical lines represent the $R_{ZZ}(\theta)$ operators, and each black square measures the spin probabilistic results.

In this application, the results of the quantum circuit are the probabilities of measuring each neuron configuration and therefore the probabilities of each neuron being active or inactive. If a neuron is active, that means it is able to send and receive signals through neurotransmitters. If a neuron is inactive, that means

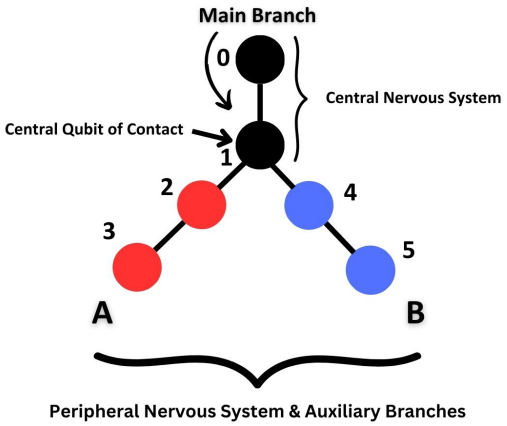

Figure 6. Hypothetical biological neural network with length 2 for simplicity. Refer back to **Figure 2** for the length 4 model analyzed in this paper.

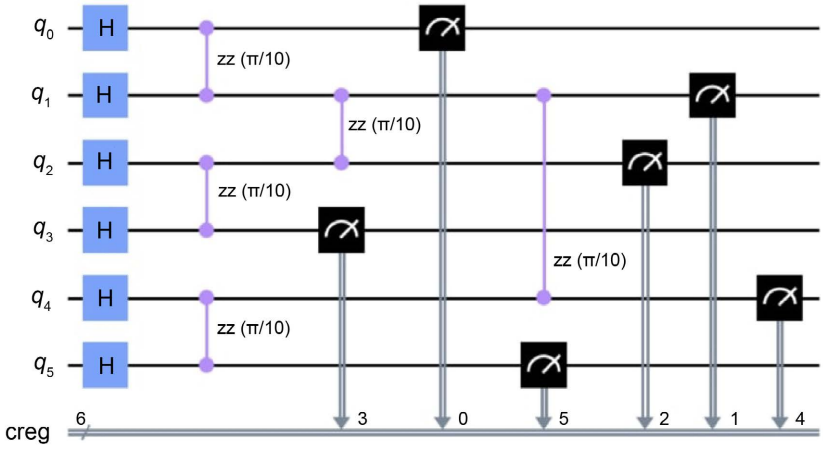

Figure 7. Hypothetical biological neural network quantum circuit with 6 neurons. Note q_1, the Central Qubit of Interaction with the most number of connections with other qubits.

it lacks the ability to send or receive signals. An active neuron is represented by a spin-up qubit denoted by 0, and an inactive neuron is represented by a spin-down qubit denoted by 1. An example of a neuron configuration (quantum state) is 010011, which shows the neurons that are measured as active or inactive and the neuron index increases from left to right.

Furthermore, notice that the qubit in **Figure 7** denoted q_1 has the most number of connections or $R_{ZZ}(\theta)$ interactions with other qubits. This means that this qubit is the Central Qubit of Interaction and the child of the Main Branch. The Central Qubit of Interaction is labeled in **Figure 6**.

Note that for this paper, we use the BNN depicted in **Figure 2**. The BNN shown in **Figure 6** is merely for example purposes.

3.3. Magnetic Material System Results

In order to classify a magnetic material as ferromagnetic (same spin direction in

the presence of external magnetic field) or paramagnetic (equal number of spin-up and spin-down electrons in the presence of external magnetic field), we need to utilize the values of J and h as metrics. Recall that J represents the coefficient of interaction between particles, and h represents the coefficient of perturbation from external magnetic fields. We determine the relationship between J and h by inputting different values of J and h (phase angles) in a particular system's quantum circuit before running it. We analyze data from a total of 10,000 shots per run.

Figure 8 measures the probability of alignment, or the probability that every electron is spin-up or spin-down, for a hypothetical magnetic material with 4 electrons. When the electrons are all aligned, the material is ferromagnetic and therefore produces the strongest electric field towards the source of the magnetic field [14]. We notice a pattern when J and h have the same sign, for instance, if the value of J is positive and the value of h is also positive, the probability of alignment is greatest. On the other hand, when J and h have the opposite sign, the probability of alignment is the lowest, and therefore the particular material would produce the weakest electric field [14].

We confirm this proposed phenomenon by analyzing bar charts that depict the number of shots for each possible spin state when J and h have the same sign or opposite sign. We ensure that the magnitudes of J and h are the same to reduce variability from extraneous factors.

Figure 9 shows that, when J and h are both positive, the spin configurations (quantum states) 0000 and 1111 have the highest number of shots out of 10,000. Likewise, when they were both negative, a similar pattern emerged. Hence, the probability of the electrons being aligned and therefore the material being ferromagnetic are likely higher when J and h share the same sign.

Figure 10 shows that, when the signs of J and h were different, in this case when J is negative and h is positive, the spin configurations 0101 and 1010 have the highest number of shots out of 10,000. Likewise, when J is positive and h is

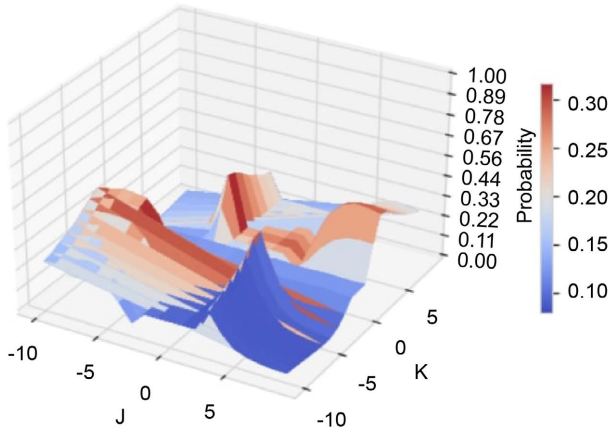

Figure 8. Coefficients J and h on the electron alignment probability. Note that when the J and h (in the graph denoted K) coefficients have the same sign, the probability of alignment is greatest.

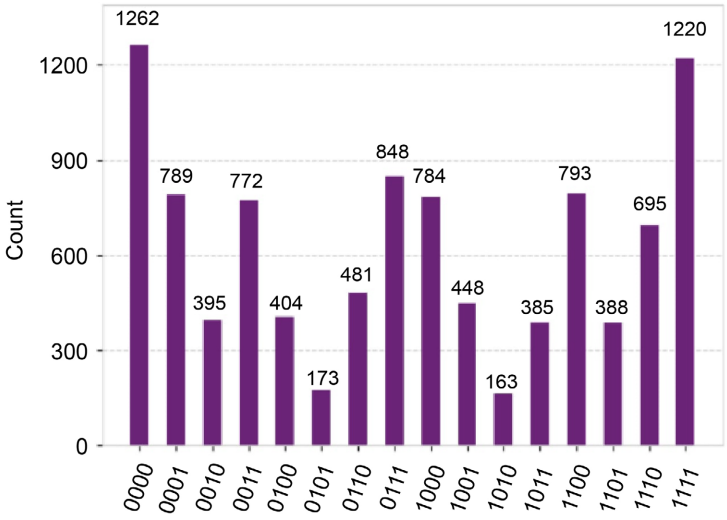

Figure 9. Ferromagnetic electron spin distribution from a sample of 10,000 shots. Note that the electron configurations of 0000 and 1111 have the highest probabilities, therefore, the electrons are most likely to be aligned.

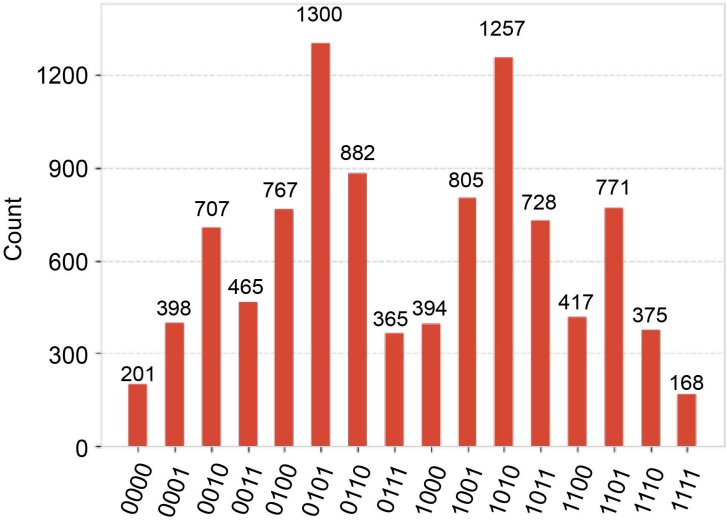

Figure 10. Paramagnetic electron spin distribution from a sample of 10,000 shots. Note that the electron configurations of 0101 and 1010 have the highest probabilities, therefore, the electrons are most likely to be misaligned.

negative, 0101 and 1010 still had the highest number of shots. Therefore, the probability of the magnetic material being paramagnetic is likely higher when J and h have opposite signs.

3.4. Neural Network System Results

The brain is composed of approximately 10 billion neurons [22]. Each neuron can be seen as a single processing unit that receives and sends electrochemical signals from one neuron to another in a chain-like process. These electrochemical signals represent the "information" that constantly transfers across all the neurons in a body known as the biological neural network [22].

One reason why neurons are important is that they allow for motor functions [23]. For example, when neurotransmitters send signals from the brain to the peripheral nervous system (other areas of the body), that area is given a command to move. However, if neurons in that path are damaged, the electrochemical signals never travel down to the area, which can lead to paralysis. In other cases, damage to neurons may cause phenomena such as the loss of feeling and sensations. Without properly functioning neurons, daily tasks such as eating, thinking, and walking are impossible [23].

Neurosurgery is commonly performed on patients who exhibit issues with existing neurons. However, surgeons are not immune to making mistakes, around 4000 surgical errors or "never events" occur in the United States annually [24].

Consequently, prior to neurosurgery, it is essential for experts to know which neurons are more valuable to the overall neural network to avoid damaging it. This section introduces a method to achieve that information with quantum computing and the Ising Model.

The value or importance of a neuron can be quantified by the neural network's information retention if that neuron is damaged or outright removed. In a BNN, we think of information retention as the amount of information remaining when an electrical signal passed in the first neuron reaches the dendrite of the final neuron [22]. When neurons are damaged, for instance during neurosurgery, neurotransmitters fail to pass from the synapse of one neuron to the dendrite of the neighboring neuron [22]. Therefore, the total information retained is reduced.

Total system information retention is quantified by entropy, which is the level of disorder in a system and therefore the information stored. Entropy can be found by evaluating the following expression:

$$S(\rho) = -trace(\rho \log \rho) \tag{12}$$

where ρ is a density matrix depicting the probabilities corresponding to each of the 2^N possible qubit spin configurations. There are 2^N possible spin configurations (or quantum states) because there are N qubits, and each qubit can be measured as spin-up (0) or spin-down (1). Hence, 2^N possible permutations [25].

Figure 11 shows the effect of removing an arbitrary number of neurons from a hypothetical neural network with 4 neurons. We see an exponential decline in total system information retention as more neurons are removed. Refer back to **Figure 2** for a detailed image of the biological neural network model we use.

To gauge the relative importance of each neuron in a biological neural network, we compare the fractions of initial entropy retained when the neurons are removed. **Figure 12** plots the percent information retained after each neuron is removed based on the model shown in **Figure 2**. The largest decrease in entropy occurs after removing Neuron 3, therefore, Neuron 3 is the most important to the neural network. This makes sense because Neuron 3 maps to the Central Qubit of Interaction. If this was a real system, experts should be aware that

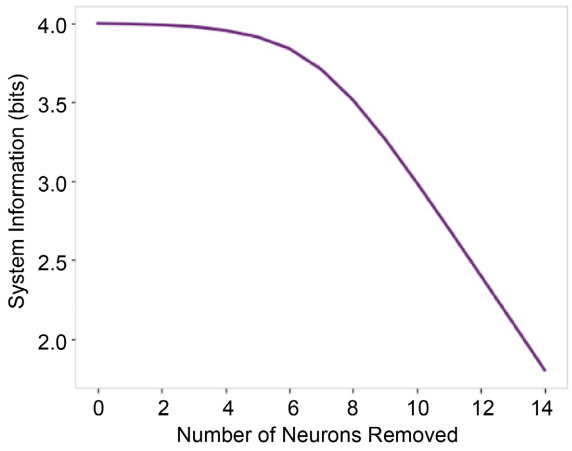

Figure 11. Number of neurons removed on system information. Note the exponential decrease in system information (entropy) as more neurons are removed.

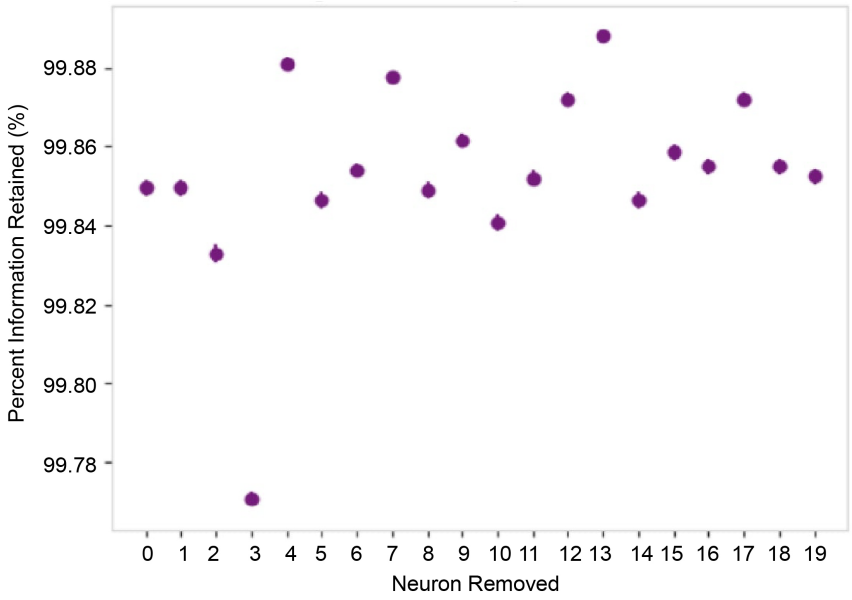

Figure 12. Specific neuron removed on system information. Note that removing Neuron 3, the Central Qubit of Interaction, correctly decreases the system information (entropy) the most.

Neuron 3 is the most important and should avoid surgery around it.

Different neural networks may vary in terms of how information is transferred from neuron to neuron, branch to branch. One possible difference between neural networks is the ratio of the length of the main branch versus the length of each auxiliary branch. Figure 13 shows the effects of changing this ratio on the entropy of the neural network. As the ratio increases, so does the entropy, albeit minimally. Occasionally, the entropy decreases, for example, when the ratio is 3.5 or 4.5. We aren't sure why entropy decreases at those values, but we are looking into possible causes. This is potentially an area for future work and analysis.

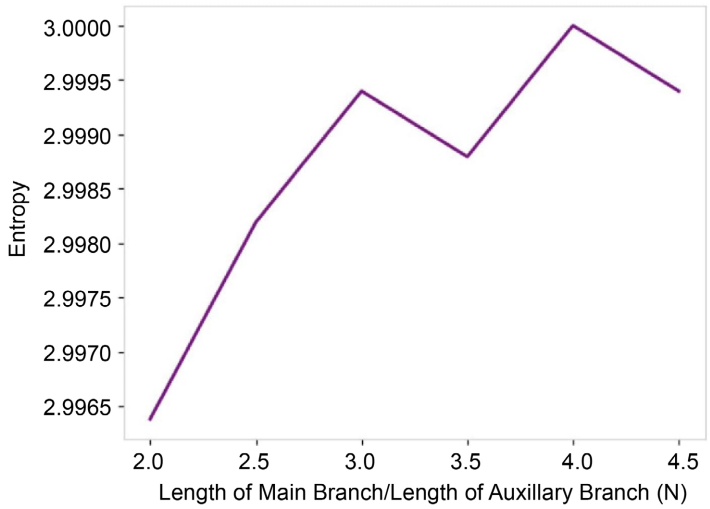

Figure 13. Length of Main Branch vs Auxiliary Branches on system information (entropy). Note the unexpected decrease in entropy at ratios of 3.5 and 4.5.

4. Conclusions & Discussion

By demonstrating our model's ability to simulate 1-D and 2-D systems, we conclude that quantum computing can be paired with the Ising Model to better model physical systems. First, we demonstrated the ability of quantum computing to classify a given material as ferromagnetic or paramagnetic based on its 1-D Ising Model configuration. We provided instances of results that accurately matched the electron alignment of ferromagnetic materials and the opposing alignment of paramagnetic materials.

While previous studies modeled magnetic materials using quantum circuits, our study expanded on previous literature by showing that the sample mathematical relationship can also be extrapolated to biological neural networks (BNNs). We computed the relative importance of each neuron in a BNN with length 4, accurately concluding that removing the Central Qubit of Interaction reduced the system entropy the most and was therefore the most important to the overall BNN. We also explored the relationship between the number of neurons removed and the ratio of the length of the Main Branch vs the Auxiliary Branches to the total system information of the BNN.

We expanded on previous literature by showing that our mathematical framework is effective at simulating basic theoretical node-based neural networks. Simulating a real-world neural network would require more complex connections and more powerful quantum computers with more qubits. Given powerful quantum computers and parameterized environmental factors, future work will be able to improve the effectiveness of neurosurgery since this approach will allow experts to simulate the effects of surgery prior to performing it. All in all, not only may our findings help experts in the field of neurosurgery, the feasibility of modeling complex 2-D tree-like BNNs demonstrates great potential regarding the intersection of the Ising Model and quantum computing.

Acknowledgements

Thank you to Dr. Fatimah Ahmadi at Oxford University for helping answer questions relating to quantum computing and giving suggestions to improve our paper during the paper writing process.

Sincere thanks to Mark Hannum, the Quantum Lab Director at Thomas Jefferson High School for Science and Technology, for sparking our curiosity in this subject and answering our questions.

Special thanks to Thomas Jefferson High School for Science and Technology (TJHSST), Fairfax County Public Schools (FCPS), and Old Dominion University for giving us the opportunity to present some of our early work at the Science Fairs.

We acknowledge the use of IBM Quantum services for this work. The views expressed are those of the authors and do not reflect the official policy or position of IBM or the IBM Quantum team.

Conflicts of Interest

The authors declare no conflicts of interest regarding the publication of this paper.

References

[1] Bogobowicz, M., Gao, S., Masiowski, M., Mohr, N., Soller, N., Zemmel, R. and Zesko, M. (2023) Quantum Technology Sees Record Investments, Progress on Talent Gap. McKinsey Digital. https://www.mckinsey.com/capabilities/mckinsey-digital/our-insights/quantum-technology-sees-record-investments-progress-on-talent-gap#/

[2] Martonosi, M. and Roetteler, M. (2018) Next Steps in Quantum Computing: Computer Science's Role. http://arxiv.org/abs/1903.10541

[3] Gamble, S. (2018) Quantum Computing: What It Is, Why We Want It, and How We're Trying to Get It. Frontiers of Engineering: Reports on Leading-Edge Engineering from the 2018 Symposium, 5-8. https://nap.nationalacademies.org/read/25333/chapter/1

[4] Bhatia, V. and Ramkumar, K. (2020) An Efficient Quantum Computing Technique for Cracking RSA Using Shor's Algorithm. 2020 *IEEE 5th International Conference on Computing Communication and Automation* (*ICCCA*), Greater Noida, 30-31 October 2020, 89-94. https://doi.org/10.1109/ICCCA49541.2020.9250806

[5] Li, J., Peng, X., Du, J. and Suter, D. (2012) An Efficient Exact Quantum Algorithm for the Integer Square-Free Decomposition Problem. *Scientific Reports*, **2**, Article No. 260. https://doi.org/10.1038/srep00260

[6] Brush, S. (1967) History of the Lenz-Ising Model. *Reviews of Modern Physics*, **39**, 883-893. https://doi.org/10.1103/RevModPhys.39.883

[7] Adelomou, A., Ribé, E. and Cardona, X. (2020) Formulation of the Social Workers' Problem in Quadratic Unconstrained Binary Optimization Form and Solve It on a Quantum Computer. *Journal of Computer and Communications*, **8**, 44-68. https://doi.org/10.4236/jcc.2020.811004

[8] Lima, F. (2022) Tax Evasion Dynamics via Ising Model Spin S = 1. *Theoretical*

Economics Letters, **12**, 400-410. https://doi.org/10.4236/tel.2022.122021

[9] Singh, S. (2020) The Ising Model: Brief Introduction and Its Application. In: Sivasankaran, S., Nayak, P.K. and Günay, E., Eds., *Metastable, Spintronics Materials and Mechanics of Deformable Bodies*, IntechOpen, London, 19.

[10] Obermeyer, J. (2020) The Ising Model in One and Two Dimensions. Seminar on Statistical Physics at the University of Heidelberg. https://www.thphys.uni-heidelberg.de/~wolschin/statsem20_3s.pdf

[11] Feiguin, A. (2009) Suzuki-Trotter Transformation and the Equivalent Classical System. Northeastern University, Boston. https://web.northeastern.edu/afeiguin/phys5870/phys5870/node103.html

[12] Zwerver, A.M.J., Krähenmann, T., Watson, T.F., Lampert, L., George, H.C., Pillarisetty, R., Bojarski, S.A., Amin, P., Amitonov, S.V., Boter, J.M., *et al.* (2009) Qubits Made by Advanced Semiconductor Manufacturing. *Nature Electronics*, **5**, 184-190. https://doi.org/10.1038/s41928-022-00727-9

[13] IBM (2021) IBM Quantum Platform. https://quantum-computing.ibm.com/

[14] Helmenstine, A. (2022) Paramagnetic vs Diamagnetic vs Ferromagnetic—Magnetism. Science Notes. https://sciencenotes.org/paramagnetic-vs-diamagnetic-vs-ferromagnetic-magnetism

[15] Jeffrey (2019) The Ising Model. https://stanford.edu/~jeffjar/statmech/intro4.html

[16] Djordjevic, I. (2022) Quantum Error Correction Fundamentals. In: Djordjevic, I.B., Ed., *Quantum Communication, Quantum Networks, and Quantum Sensing*, Elsevier, Amsterdam, 273-312. https://doi.org/10.1016/B978-0-12-822942-2.00003-0

[17] Aleksandrowicz, G., Alexander, T., Barkoutsos, P., Bello, L., Ben-Halm, Y., Bucher, D., Cabrera-Hernández, F.J., Carballo-Franquis, J., Chen, A. and Chen, C. (2023) Qiskit: An Open-Source Framework for Quantum Computing.

[18] Yang, X., Nie, X., Ji, Y., Xin, T., Lu, D. and Li, J. (2022) Improved Quantum Computing with Higher-Order Trotter Decomposition. *Physical Review A*, **106**, Article ID: 042401. https://doi.org/10.1103/PhysRevA.106.042401

[19] Cases, F., Murua, A. and Nadinic, M. (2012) Efficient Computation of the Zassenhaus Formula. *Computer Physics Communications*, **183**, 2386-2391. https://doi.org/10.1016/j.cpc.2012.06.006

[20] Gould, H. and Tobochnik, J. (2009) Thermal and Statistical Physics. https://press.princeton.edu/books/hardcover/9780691201894/statistical-and-thermal-physics https://doi.org/10.1515/9781400837038

[21] Bundy, A. and Wallen, L. (1984) Breadth-First Search. In: Bundy, A. and Wallen, L., Eds., *Catalogue of Artificial Intelligence Tools*, Springer, Berlin, 13. https://doi.org/10.1007/978-3-642-96868-6_25

[22] Clabaugh, C., Myszewski, D. and Pang, J. (2000) Neural Networks. https://cs.stanford.edu/people/eroberts/courses/soco/projects/neural-networks/index.html

[23] National Institute of Neurological Disorders and Stroke (n.d.) Brain Basics: The Life and Death of a Neuron. https://www.ninds.nih.gov/health-information/public-education/brain-basics/brain-basics-life-and-death-neuron

[24] Nordqvist, J. (2012) Surgical Errors Occur More than 4,000 Times a Year in the U.S. Medical News Today. https://www.medicalnewstoday.com/articles/254426#1

[25] Nielson, M.A. and Chuang, I.L. (2010) Quantum Computation and Quantum Information. Cambridge University Press, Cambridge.
https://cds.cern.ch/record/465953/files/0521635039_TOC.pdf